



Cite this: *Lab Chip*, 2014, 14, 4415

An integrated sample-in-answer-out microfluidic chip for rapid human identification by STR analysis†

Delphine Le Roux,^{‡a} Brian E. Root,^{‡b} Jeffrey A. Hickey,^b Orion N. Scott,^b Anchi Tsuei,^b Jingyi Li,^b David J. Saul,^c Luc Chassagne,^a James P. Landers^{§d} and Philippe de Mazancourt^{§*a}

A fully integrated microfluidic chip for human identification by short tandem repeat (STR) analysis that includes a unique enzymatic liquid preparation of the DNA, microliter non-contact PCR, and a polymer that allows a high-resolution separation within a compact microchip footprint has been developed. A heat-activated enzyme that digests biological materials is employed to generate the target yield of DNA from a buccal swab or FTA paper. The microfluidic architecture meters an aliquot of the liberated DNA and mixes it with the PCR reagents prior to non-contact IR-mediated PCR amplification. The products of PCR amplification are mixed with a sizing standard (ladder) and the 18-plex STR amplicons are separated in an effective length (L_{eff}) of just 7 cm. The development, optimization and integration of each of these processes within the microfluidic chip are described. The device is able to generate genetic profiles in approximately 2 hours that match the profiles from the conventional processes performed using separate conventional instruments. Analysis is performed on a single plastic microchip with a size similar to that of a 96-well plate and only a few mm thick with no pretreatment of any of the functional domains. This is significant advancement in terms of ease of fabrication over glass microdevices or polymeric systems assembled from multiple components. Consequently, this fully integrated sample-in-answer-out microchip is an important step toward generation of a rapid micro-total analysis system for point-of-collection human identification based on genetic analysis.

Received 11th June 2014,
Accepted 1st September 2014

DOI: 10.1039/c4lc00685b

www.rsc.org/loc

1. Introduction

The last few decades have seen extensive research into the development of micro-total analysis systems (μ -TAS) for genetic analysis and diagnostics.^{1–6} The microfluidics field offers a large number of advantages for rapidly analyzing samples, primarily because several steps commonly performed using different benchtop instruments can be integrated into single microfluidic or ‘lab-on-a-chip’ devices.⁷ The entire sample

processing often encompasses: (1) sample collection and treatment to release the target of interest (*e.g.*, bacteria, DNA, proteins, cell), (2) amplification of the target and (3) detection and interpretation of this amplification product to generate the result of the assay. Many of these benchtop processes have been independently demonstrated on microfluidic chips.^{8–11} When performed in a conventional laboratory, these steps require trained technicians to transfer the samples to the instruments performing each of the different steps and are frequently performed in batches that lead to a long turn-around time. Additionally, current benchtop analytical processes are often long, and contamination can occur because samples are transferred from one tube to another between steps. Some efforts have been made to try to automate benchtop processes,¹² but microfluidic devices may offer a greater possibility of faster sub-assay times and automated integration of multiple processes. However, realizing this vision of integrating multiple steps has been challenging, especially when it comes to integrating sample preparation.^{13,14}

Demonstrations of integrated microfluidic analysis systems have varied widely in terms of the target and the analytical detection method (*e.g.*, qPCR, electrophoresis,

^a Versailles – Saint Quentin en Yvelines University, 55 Avenue de Paris, 78000 Versailles, France. E-mail: philippe.de-mazancourt@uvsq.fr; Fax: +33139274535; Tel: +33139274287

^b MicroLab Diagnostics, Inc, 705D Dale Ave, Charlottesville, VA 22903, USA

^c ZyGEM Corporation Ltd, Waikato Innovation Park, Ruakura Road, Hamilton 3216 Aotearoa, New Zealand

^d Departments of Chemistry, Mechanical Engineering and Pathology, University of Virginia, Chemistry Drive, Charlottesville, VA 22904, USA

† Electronic supplementary information (ESI) available: Microfluidic chip fabrication, sample collection, analytical processes inside the microfluidic chip, conventional analysis, instrument modules, data analysis, aliquot line volume and supplementary figures. See DOI: 10.1039/c4lc00685b

‡ These authors contributed equally to this work.

§ These authors contributed equally to this work.

colorimetric, *etc.*).^{15–24} While qPCR has begun to dominate, many genetic assays still require electrophoretic separation to provide the assay output. One such assay requiring electrophoretic separation is forensic short tandem repeat (STR) analysis for human identification.²⁵ This assay is particularly challenging for integrated microfluidics as it has very stringent requirements and requires at least three analytical steps: (1) DNA preparation from the sample, (2) DNA amplification, and (3) DNA separation with multicolour fluorescence detection.²⁶ Often, the reagents used for one of these steps are incompatible or detrimental to downstream processes, which further increases the complexity of the microfluidic architecture in order to isolate any incompatible reagents.²⁷

The first demonstration of a sample-in-answer-out microfluidic chip for genetic analysis by Easley *et al.*²⁷ detected *B. anthracis* from blood by solid-phase extraction, PCR, and electrophoretic separation. However, several limitations of this system, such as single-color detection and separation resolution, make it non-applicable to STR analysis. Liu *et al.*²⁸ expanded on this work to demonstrate an integrated microchip for STR analysis. While the level of assay integration is significant, the complex microchip is manufactured from glass and requires pre-treatment of the channel (*e.g.*, polymer-coating the separation channel), which make this approach prohibitively expensive for widespread use.

Other systems have been demonstrated in recent years, each with advantages and limitations. Two groups working toward point-of-collection STR analysis demonstrated end-to-end analysis, but with the electrophoretic separation performed on either a separate separation microchip or a capillary.^{29,30} This arrangement results in multiple consumable components and does not fulfill true μ TAS system criteria. Another demonstration of an integrated chip required a relatively large footprint (296 mm \times 166 mm) with the device being an assembled multi-component structure.³¹ The result is a bulky device that requires complex and expensive manufacturing. While each of these systems represents significant advancement for STR analysis, taken together, their limitations demonstrate the challenge of creating a compact, low-cost, fully integrated disposable microchip for this type of assay.

Here, we report on the development of an integrated microfluidic chip for ‘sample in-answer-out’ human identification that is a single injection-molded device similar in size to a 96-well plate with simple, low-cost fabrication. Contributing to the compact size is the direct DNA liberation using the protease from *Bacillus sp. Erebus antarctica* 1 (EA1)^{32,33} that circumvents washing steps, a small PCR chamber heated by an IR laser³⁴ and a 7 cm microchannel capillary containing a unique, self-coating polymer for DNA separation. Moreover, the microfluidic chip is completely self-contained: following sample input, no liquids can enter or exit the microchip during the assay and the instrument itself is not directly in contact with any liquid, minimizing the risk of contamination. Uniquely, the extracted DNA and amplified products are easily recoverable for conventional post-assay analysis if desired. The total assay time is

reduced to almost 2 hours compared to the conventional processes in a forensic laboratory of up to 10 hours.

The instrument driving the functions on the microfluidic chip has embedded hardware that controls fluid flow from sample input to 5-color fluorescence read-out of each of four samples. As a means of minimizing microdevice complexity and cost, the chip contains no active, functional features (*e.g.*, resistive heaters, temperature sensors, complex valving schemes such as one-way or phase-change valves), which allows this design to be easily fabricated. In this paper, we demonstrate the utility of each sub-assay (Liquid Extraction (LE), Powerplex® 18 Fast System PCR and Microchip Electrophoresis (ME)) as well as the integration of two of the sub-assays together (*i.e.* LE-PCR and PCR-ME) to finally achieve the full integration of the process. For the first time, the full functionality of the integrated microchip and instrument is demonstrated, giving credence to the value of multiprocess microfluidic integration into a system that has the potential for low-cost manufacturing.

2. Methods and experimental section

2.1. Microfluidic chip design

Previous work has shown that PCR and separation can be integrated for forensic STR analysis on a plastic microfluidic chip with the dimensions of a 96-well plate.³⁵ The plastic microfluidic chip demonstrated here completes the fully integrated process of DNA liquid extraction, aliquoting a volume of the DNA extract, mixing with PCR reagents, PCR, and electrophoretic separation with embedded electrodes – all within a completely enclosed disposable chip. The additional assay processes, as well as reagent metering and mixing, significantly increase the complexity of the microfluidic chip design. Therefore, the injection-molded chip has features on both sides (top and bottom), creating two layers to achieve this additional functionality while retaining a minimal footprint. These two layers are a fluidic layer, containing many of the reagent storage reservoirs and transport channels, and an analytical layer, containing the PCR chamber and separation channel. The analytical layer also contains some transport channels by necessity of design. This is described in more detail in the ESI.†

Fig. 1a and b shows a schematic of the chip design and an image of a filled chip, respectively. Development of individual components of the design is discussed in the results section with respect to verifying functionality such as reagent mixing and DNA extract volume. Fig. 1a identifies each of the critical microfluidic features described in the following discussion. Fig. 1b shows the bottom side of the chip, which is transparent to allow non-contact PCR and laser-induced fluorescence detection. The top of the cartridge physically interacts with several components of the instrument for flow control and for electrical interface. The pneumatic interface allowing the pressure-driven fluid movement within the microchip is covered with a hydrophobic membrane (PTFE, 0.2 micron, Sterlitech, Kent, WA, USA) to prevent liquid from

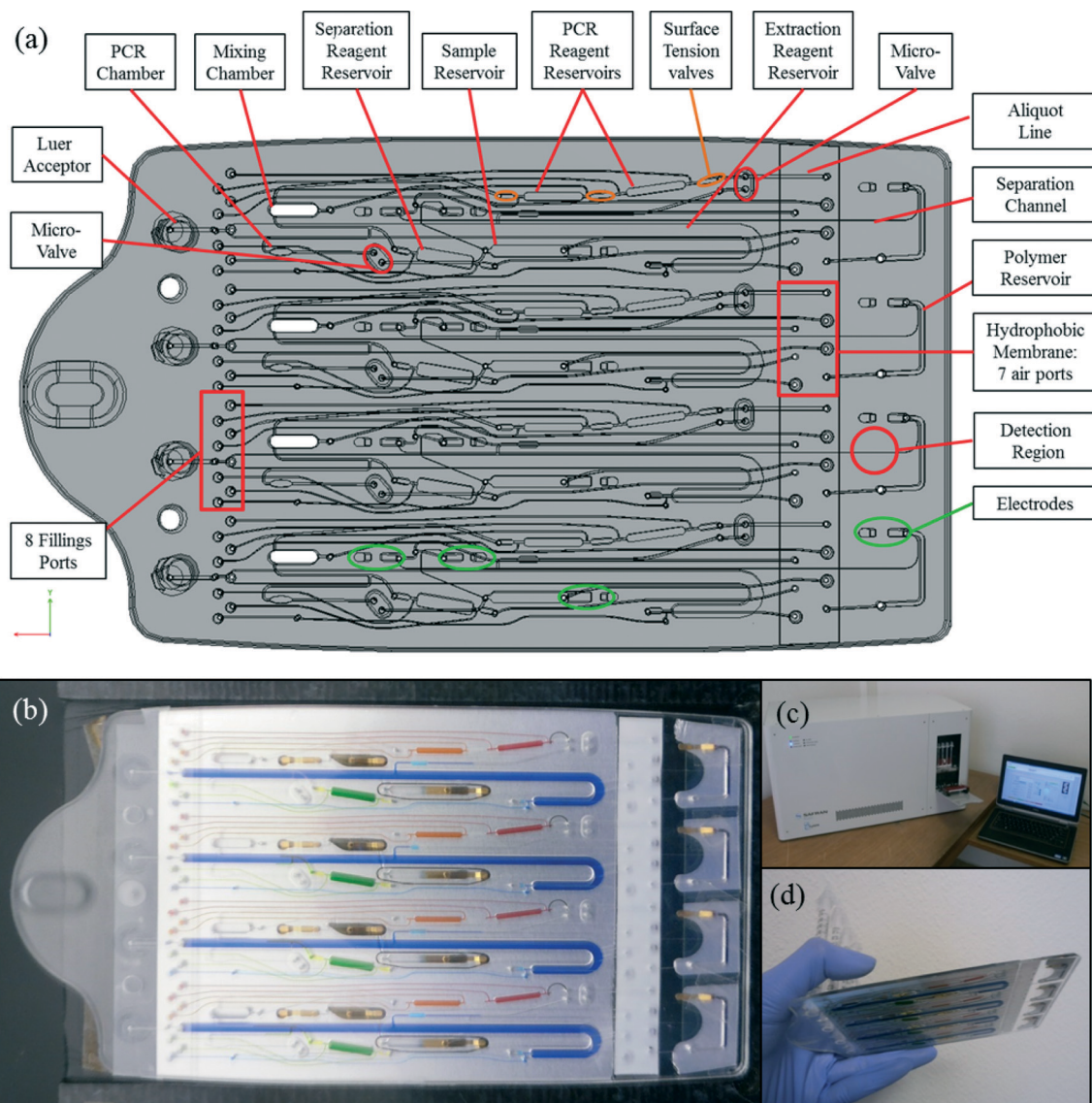


Fig. 1 Microfluidic chip for “sample-in-answer-out” integrated DNA processing. (a) Schematic representation of the microchip with major microfluidic features. (b) Bottom view of the cartridge containing the fluidic layout with blue reagents in the extraction reagent reservoir, red and orange reagents in the PCR reagent reservoirs, green reagents in the separation reagent reservoir and polymer in the polymer reservoir. (c) Microchip inside the instrument enabling its functionality with swabs attached and computer for software control. (d) View of the microchip with swabs attached to it with a hand scale.

getting in contact with the instrument Chip Interface Module (CIM). The functions of the other microfluidic features highlighted in Fig. 1a are described in the discussions below.

Fig. 1b shows the integrated chip filled with dye to highlight each of the reagent reservoirs. The reservoirs and their volumes are given in Table 1. The loading volumes are different because the filling lines from where the liquids are introduced into the chip are different for each of the reservoirs (the liquids are introduced from the filling ports highlighted by a red box in Fig. 1a). After reagent loading, four sample collectors are attached to this disposable device (Fig. 1d) and inserted into the CIM (Fig. 1c). The instrument door is closed, locking the chip inside, and a main piston brings the CIM down into contact with the chip.

2.2. Instrument design

Fig. 1c shows the instrument that drives the analysis within the microfluidic chip. The main features interacting with the microfluidic chip (shown in Fig. 1b) are located within the Chip Interface Module (CIM) which is designed to receive

Table 1 Reagent volumes inside the microchip reservoirs and dye colors corresponding to each shown in Fig. 1b

Reagent reservoir	Color	Volume (μl)
Extraction reagents	Blue	200
PCR mix #1	Red	5.5
PCR mix #2	Orange	5.5
Separation reagents	Green	17
Polymer	Purple	20

the microfluidic chip with the sample acceptors attached (Fig. 1d). An important component of this module is an air supply system that meters different volumes with controllable flow rates to seven different ports per channel that are linked to specific chambers and channels to control the fluidic movements. A silicon gasket that mates with the pneumatic interface region of the microchip allows air distribution from a syringe pump (54848-01-LMZ, Hamilton Company, Reno, NV, USA) with a 250 μL syringe (57252-01, Hamilton Company) used to create positive or negative pressure to drive the fluidics. The syringe pump is connected to a manifold that uses high-density 3-way solenoid valves (LHDA 1223111H, The Lee Company, Westbrook, CT, USA) to direct the pressure to one or more of the seven ports on each channel. Two additional pneumatic pistons per channel are needed for additional fluidic control by microfluidic valves (Fig. 1a). Other instrument modules are described in the ESI.†

2.3. Microfluidic chip loading

The reagent reservoirs are filled by pipetting into the filling port of each reservoir (Fig. 1, 2 filling ports per reservoir, 8 in total per channel). Once the reagents are loaded, the filling area is sealed with a pressure-sensitive adhesive (PSA) strip (Adhesives Research, Glen Rock, PA, USA). The separation polymer is loaded to the polymer reservoir to the right of the detection zone in Fig. 1a and is sealed with a PSA.

Microfluidic chip loading for a complete integrated run comprises the following steps: (1) adding a volume greater than 200 μL to ensure complete filling of the reservoir and filling channels of the extraction reagents. A total of 900 μL is prepared for four channels to allow extra volume for pipette errors: 846 μL of extraction buffer and 54 μL of EA1 enzyme based on the prepGEM™ Saliva kit (ZyGEM Corp., Hamilton, New Zealand). (2) Thirteen μL of PCR reagents is used to fill both PCR reservoirs. PCR reagents are prepared with the PowerPlex® 18 Fast System (Promega Corp., Madison, WI, USA): 69 μL of Promega PowerPlex® 18 Fast System primers, 35 μL of Promega PowerPlex® 18 Fast System reaction mix and 6 μL of water. The Promega primer and reaction mix were modified by Promega for this specific PCR (based on the PowerPlex® 18D System).³⁶ (3) The separation reservoir is filled with 25 μL of a separation reagent mix of 18 μL of Internal Lane Standard (ILS) 500 (Promega) and 90 μL of dilution buffer (Hi-DI™ Formamide, Life Technologies, Carlsbad, CA, USA) prepared for four channels. (4) Finally, 20 μL of hydrophobically modified polyacrylamide polymer³⁵ (MicroLab Diagnostics Inc, VA, USA) containing a DY-680 far-red excitation dye (Dyomics GmbH, Jena, Germany) is introduced directly to the polymer reservoir. After reagent loading, four sample collectors are attached to this disposable device (Fig. 1d) and inserted into the CIM (Fig. 1c). The instrument door is closed, locking the chip inside, and a main piston brings the CIM down into contact with the chip.

For an allelic ladder separation, both PCR reservoirs are filled with water and 25 μL of separation reagents—allelic

ladder mix is introduced into the separation reagent reservoir (90 μL of Hi-DI™ Formamide, 18 μL of Internal Lane Standard 500 and 25 μL of PowerPlex® 18D allelic ladder).

2.4. Process optimization

Each of the sub-assays (LE, PCR and ME), fluidic movement from one step to the next, and sub-integration of LE-PCR and PCR-ME were tested to verify and optimize functionality. Fluidic movement tests, such as mixing, were initially evaluated based on colorimetric results and then verified with the assay result. For these sub-assay and sub-integration tests, only a portion of the microchip is loaded – the optimization approach here refers to the chip loading step numbers above.

For DNA extraction tests, only chip loading step (1) was introduced into the chip. This assay modifies the published protocol³² by reducing the enzyme activation time at 75 °C and deactivation time at 95 °C to 2 minutes each; the extraction temperature is reduced for these unique two steps, yielding PCR-ready extract. Parameters such as enzyme activation time and mixing could then be varied compared to the recommended protocol for the prepGEM Saliva kit. Two DNA sources were tested: buccal swabs (MasterAmp™ Buccal Swab Brush, Epicentre, Madison, WI, USA) and FTA™ mini card (Indicating FTA™ Mini Card, Whatman Inc., Clifton, NJ, USA). Sample collection details can be found in the ESI.† Different sample sizes of FTA were tested for the optimization step (25 mm², 50 mm², 75 mm², 100 mm² and 125 mm² out of 490 mm² for the entire FTA mini card circle). Four repeats were performed. These pieces were introduced into the 1 mL syringe attached to the chip and pushed toward the lower part to be in contact with the LE heater.

For LE-PCR, (1) and (2) were loaded. PCR test chip filling is based on the PCR mix described for PCR-ME with an appropriate volume of DNA (extracted from benchtop extraction) corresponding to the aliquot portion within the mix. To verify the PCR-ME process, the same PCR mix was introduced into the PCR chamber. Reagents (3) and (4) are filled, as previously described. PCR and ME protocols are described in the ESI.†

In the system described here, the polymer is pneumatically loaded into the microchannel by the instrument. As the polymer is loaded through the separation channel on the bottom layer of the chip and comes up through the vias, the liquid comes into contact with the electrodes almost immediately upon entering the buffer and sample waste reservoirs, resulting in connectivity between the electrodes. Additional polymer is pushed into these reservoirs to provide buffering capacity for electrophoresis. This optimization was done by observing initial connectivity over several chips and applying an additional time for polymer loading beyond this.

To assist with the fluidic movement to the sample reservoir, the current between the sample electrode and the buffer electrode was monitored. As the sample electrode (Fig. 1a) is located in the second half of the sample reservoir from where the sample enters, an increase in current between the sample and the buffer electrodes provides an indicator for fluid flow.

This is used as an active feedback sensor in the instrument control software for fluid flow to this reservoir to ensure adequate fluidic movement to the sample reservoir.

Data analysis of the STR profiles is described in the ESI.†

3. Results

3.1. Extraction optimization

The microfluidic chip, containing the extraction reagents, is fluidically connected to the sample acceptors. The pneumatic module pushes the extraction reagents from one port into the sample collector, as shown in Fig. 2a (blue-dyed reagents into the collector for all four channels). The liquid extraction reagents are then in contact with the sample within the sample collector and the temperature-based DNA liberation occurs. The contact heaters (red in Fig. 2a), contained in the CIM, clamp the sample collector to heat the extraction solution to the required temperatures. Following the LE, the solution is drawn back into the extraction reservoir.

DNA was extracted from two different sources – a brush buccal swab and FTA paper. The extraction protocol was first optimized for a buccal swab. Initial extractions pumped the liquid extraction reagents into the sample acceptor, heated the solution to the target activation and denaturation temperatures, and drew the solution out of the sample acceptor. This “simple flow” protocol resulted in an average DNA yield of $2.5 \text{ ng } \mu\text{l}^{-1}$ (Fig. 2b), which is below the yield that will produce full STR profiles in microchip PCR amplifications. Longer extraction times were tested but did not increase the yield (Fig. S2†).

Mixing after the denaturation step was tested to determine if a higher DNA yield will be obtained when the extract is pumped in and out of the sample acceptor. Doing so increased the yield by three-and-one-half times. The yield was flow rate dependent, with slower mixing ($\sim 3.5 \text{ } \mu\text{l s}^{-1}$) yielding $6.0 \text{ ng } \mu\text{l}^{-1}$ and faster mixing (approximately $15 \text{ } \mu\text{l s}^{-1}$ in and $30 \text{ } \mu\text{l s}^{-1}$ out) yielding $9.0 \text{ ng } \mu\text{l}^{-1}$. In the final protocol, the syringe compression rate was set to $50 \text{ } \mu\text{l s}^{-1}$, which yielded a fluid flow rate of approximately $20 \text{ } \mu\text{l s}^{-1}$. The difference in the syringe rate and the fluid flow rate is due to compressibility of air and air flow restrictions in the instrument between the syringe and the chip. The fluid flow rate is the critical factor and therefore the factor that is of primary interest for development.

FTA paper optimization began by testing different punch sizes of FTA mini cards (as described in section 2.4) and performing the same LE protocol as buccal swab with mixing. The PCR-ready extracts from the two smallest FTA punches did not give full conventional profiles, indicating insufficient DNA yield. The largest FTA punches gave full conventional profiles but the FTA paper absorbed too much liquid to be able to draw back a sufficient amount to have the liquid proximal to the aliquot line, which would have resulted in a failure of LE-PCR on chip. The 100 mm^2 FTA paper pieces were able to give full conventional profiles and the amount of liquid absorbed was acceptable for the aliquot step, with

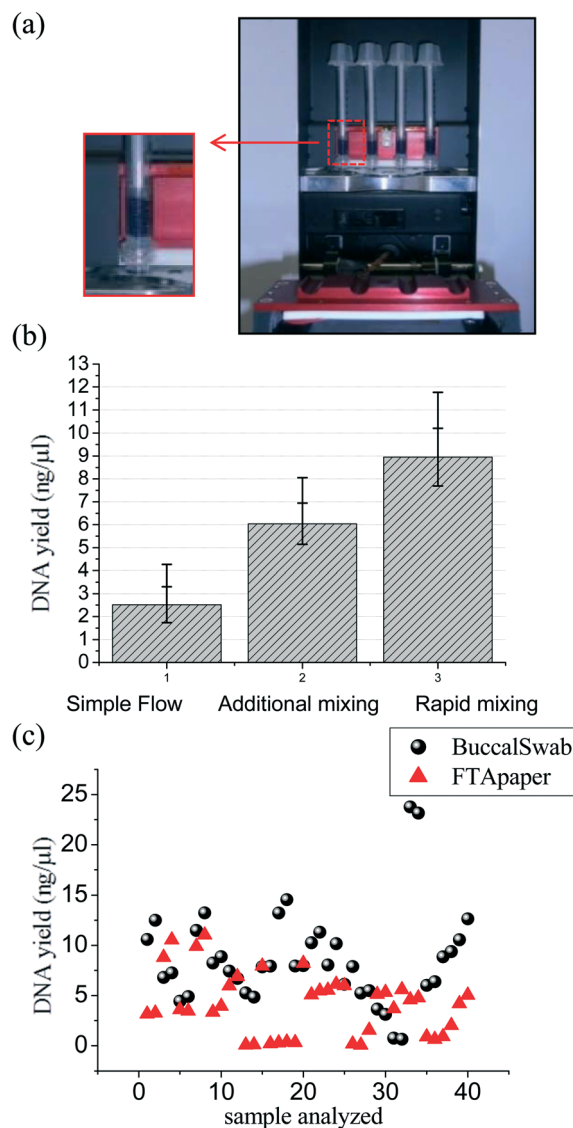


Fig. 2 Liquid Extraction on chip (LE). (a) Microchip inside the instrument with swabs submerged in blue reagents, LE occurs inside the sample acceptor tubes. (b) This graph shows the DNA yield from the LE microchip based on different fluid flow protocols to increase the DNA yield ($n = 5$). Simple flow is when the extraction mix is pushed into the syringe, heating occurs, and the fluid is simply drawn back into the microchip. Additional mixing and rapid mixing refer to additional fluid flow movements into and out of the syringe after LE heating at different rates. (c) FTA paper DNA yield compared to brush swab DNA yield using the same LE protocol on the device (20 samples for each DNA source), duplicate quantification for each sample using the Quantifiler® Duo DNA Quantification kit (Life Technologies).

a small modification of the fluid flow script, taking the absorbed liquid into account.

Confirmatory tests were done with 20 samples of 100 mm^2 FTA paper punches in parallel with 20 samples of buccal brush swab to allow direct comparison (4 donors repeated 5 times). The extracted DNA was then quantified using a Quantifiler® Duo DNA Quantification kit (Life Technologies). The yield from the FTA paper was found to be lower than

that from the buccal swabs for some of the data points (Fig. 2c). However, inhibition in the qPCR assay was observed for some of these samples, which may have resulted in this reduction. Moreover, the sample recovery and sample collection process difference can lead to variability in the results. The graph also shows that the DNA yield from the FTA paper can be as high as that obtained from the buccal swabs (for example, points around $10 \text{ ng } \mu\text{L}^{-1}$) when only 100 mm^2 of the FTA paper is put into the system compared to a buccal swab. More importantly, despite the difference in DNA yield, all samples from both the FTA paper and buccal swabs gave full profiles using the PowerPlex® 18 Fast System on a conventional PCR system (see representative full profiles in Fig. S3a and b†). Analysis of these full profiles shows that the PCR quality from both methods is comparable. Assuming that the height of each peak reflects the number of copies of the microsatellite present in the DNA (*i.e.* DNA concentration for PCR), Fig. S3c and d† show that the DNA concentration used for PCR from both methods was comparable since the peak heights fall within the same range for all of the samples. The Powerplex 18 PCR did not appear to suffer from the inhibition seen in some qPCR results. Moreover, the peak height ratio is greater than 50% for almost all of the samples (Fig. S3e†) although buccal swabs' peak height values are a little lower for some of the samples. The LE extracts from both sample types were able to provide extracted DNA samples, yielding balanced multiplexed PCR for human identification and 100% full profiles.

3.2. PCR and LE-PCR optimization

Microchip PCR has been previously demonstrated on a simpler microchip that required the preparation of extracted DNA and mixing of reagents outside the chip.³⁵ Therefore, the first step to achieve LE-PCR is to demonstrate that a DNA aliquot, with the target yield, can be microfluidically mixed with PCR reagents and flowed into the PCR chamber. An aliquot is taken by drawing the extract from the extraction reagent reservoir toward the hydrophobic membrane, as shown by the red arrows in Fig. 3a and d. The aliquot volume is defined by the aliquot line (see Fig. 1a) dimensions between the hydrophobic membrane port and the microvalve and is $4 \mu\text{L}$, as determined in preliminary studies described in the ESI.†

The microvalve is then actuated after the aliquot is taken. To prevent PCR reagents from being drawn toward the hydrophobic membrane, surface tension valves are placed on either side of the PCR reagent reservoirs (as shown in Fig. 1a). The aliquot is then pushed off the hydrophobic membrane toward the PCR reagent mixing chamber through the PCR reagent chambers (Fig. 3b and d). The DNA aliquot begins mixing with the PCR reagents during the movement to the mixing chamber. Air is pushed into the chamber to completely mix the PCR reagents and the DNA sample. Colorimetric tests indicate good mixing within this chamber (Fig. 3b).

The valve downstream of the PCR chamber is then allowed to open and the PCR mix is pushed from the mixing chamber

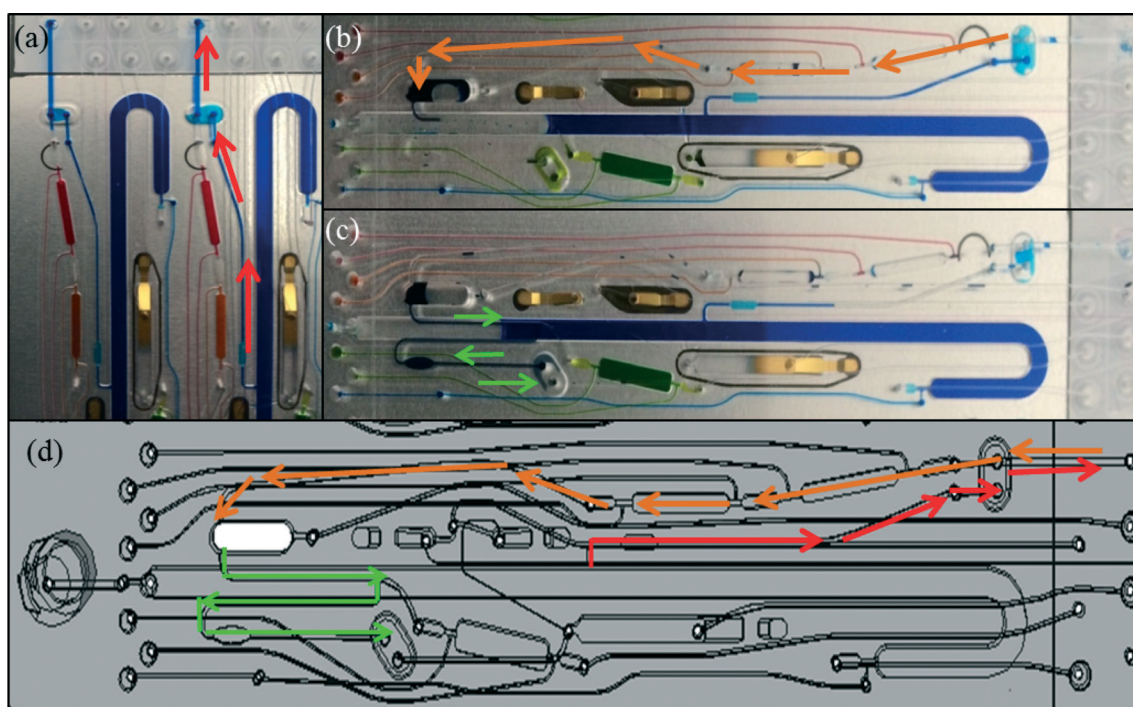


Fig. 3 LE-PCR optimization. (a) PCR-ready LE DNA aliquot drawn back from the extraction reagent reservoir toward the hydrophobic membrane. (b) Aliquot pushed toward the mixing chamber through the PCR reagent reservoirs. (c) PCR chamber filled with the PCR mix pushed toward the microvalve and stopped at it. (d) Schematic of the fluid flows during the LE-PCR: red lines for aliquoting shown in (a), orange lines for the movement to the mixing chamber shown in (b) and finally green lines for the movement from the mixing chamber to the PCR chamber shown in (c).

to the PCR chamber (Fig. 3c and d). Once the PCR chamber is filled, the microvalve downstream of the PCR chamber is closed. The PCR chamber is then pressurized to 5 psi against the microvalve to prevent bubble formation and liquid movement during PCR.

The microfluidic movement and mixing efficiency during LE-PCR were verified by comparing integrated results with a microchip amplification in which the DNA extraction and reagent mixing steps were performed off-chip. Fig. S4a and b† show LE-PCR electropherograms from a buccal swab and FTA paper, respectively. Each method produced a full profile (18-loci), characterizing a successful amplification, with similar peak balances and similar peak heights (small variations due to sample-to-sample variation and amount of the unreacted master mix pulled from the chip with the sample). The data quality of these LE-PCR tests is similar to that of PCR only on chip (off-chip mixing). Thus, these LE-PCR tests demonstrated that the microchip fluidic control is capable of generating sufficient DNA, drawing an aliquot of the extracted DNA, mixing with the PCR reagents, and filling the PCR chamber without bubbles.

3.3. Automated alignment

The separation channels have a width of 50 μm and therefore the detection sensitivity is expected to have a low tolerance to variations in chip-to-chip alignment. Fig. 4a (bars) shows the standard deviation of the alignment position for 19 chips. This variation in microchannel position from one chip to the next is then compared with the change in detection sensitivity to alignment position. Fig. S5† shows that to maintain 80% of the maximum signal, the allowable deviation in the Y axis and Z axis is approximately 10 μm and 38 μm , respectively. The lines in Fig. 4a represent this allowable deviation. While the Z axis conforms to this threshold for three out of four channels, the Y axis is well above the maximum allowable deviation. Therefore, an automated alignment method for every chip is required to detect the fluorescent DNA. To achieve this, a high-wavelength dye, outside of the dye spectrum used for the DNA, was added to the separation buffer. This dye is excited and collected by the same laser-induced fluorescence system as for the STR DNA fragments. The optics system rasters the focusing and collecting lenses in the Y axis with step changes in the Z axis (focusing axis) between lateral scans. The high-wavelength dye signal is maximized to find the separation channel. Fig. 4b shows a representative trace of the high-wavelength dye signal during the alignment procedure with the fitting curve to identify the optimal alignment point.

3.4. ME and PCR-ME optimization

Prior to ME, the polymer reservoirs are pressurized to 30 psi (see Fig. 5a and c for the polymer movement with the red arrows) to push the polymer through the separation channels to each of the buffer, sample and sample waste electrodes.

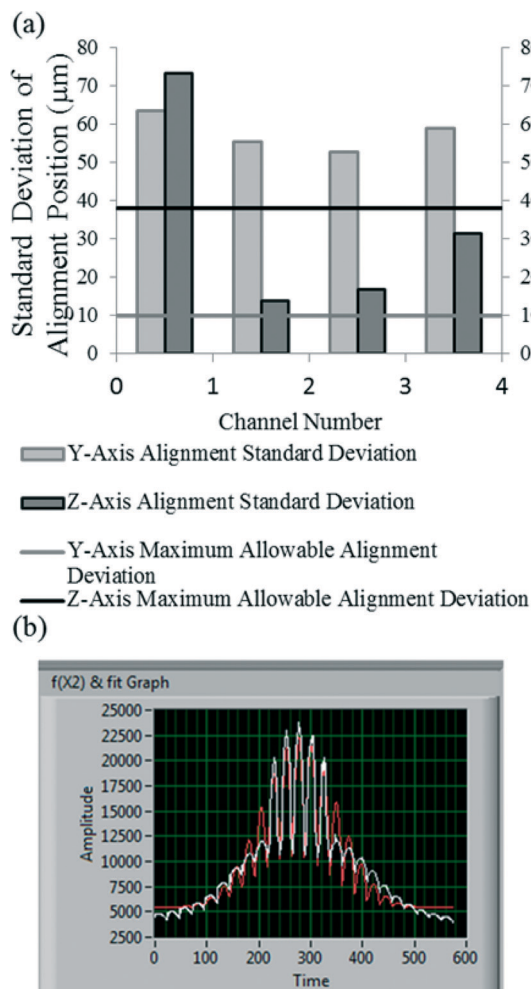


Fig. 4 Automated alignment. (a) Standard deviation of the channel alignment position over 19 microchips for the Y and Z axes for each channel (bars) compared with the maximum allowable alignment deviation to maintain 80% of the maximum signal (lines). (b) Example of an automated alignment result in which the optics are rastered in the Y axis and incrementally moved in the Z direction around the expected alignment position. The graph shows the fluorescence intensity of the high-wavelength dye over the time of the scan (white line) and a line from a fitting algorithm (red line) that determines the correct alignment position.

This loading pressure was applied for 30 minutes in addition to connectivity time to allow excess polymer to provide buffering capacity to the buffer and sample waste electrodes for stable electrophoresis current during the entire separation process. The polymer loading time can be decreased if the loading pressure is increased or if the polymer viscosity is decreased. However, this polymer loading step was performed during the PCR in the PCR-ME and the full integrated runs; therefore it fits well within the process flow of the chip assay.

After PCR thermocycling, the PCR chamber pressure is slowly released and the microvalves are opened. Separation buffer is pushed through the PCR chamber into the separation sample reservoir with current assistance, as described in section 2.4. The orange arrows in Fig. 5b and c show the

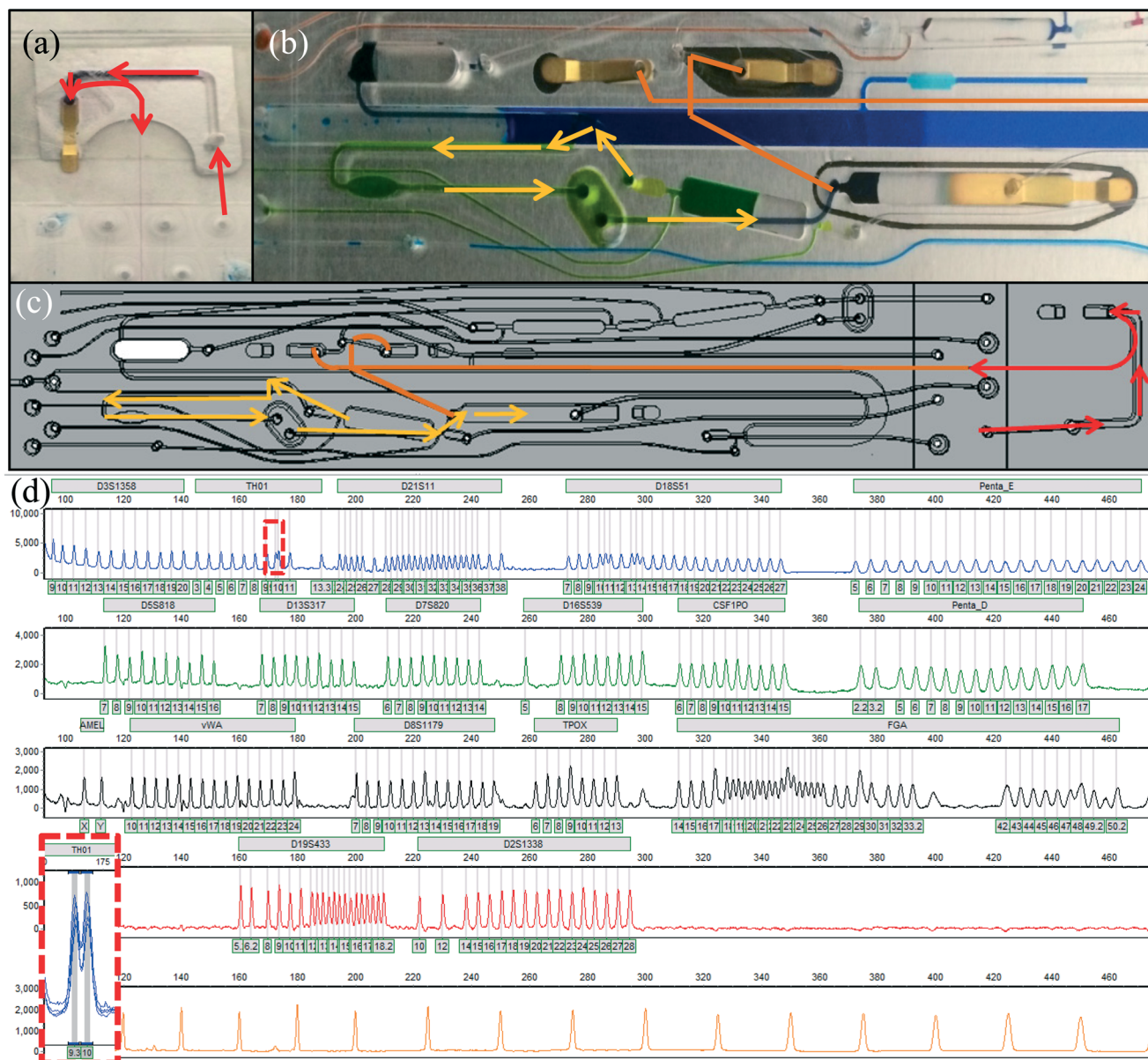


Fig. 5 PCR-ME optimization. (a) Polymer filling the microchip electrophoresis separation channel. (b) Separation reagents moving through the PCR chamber toward the sample reservoir, flushing the PCR products. Red arrows show the fluidic movement. The PCR products mixed with the separation reagents are then ready to be electrophoretically separated (cross T injection and separation microchannel shown in orange). (c) Schematic view of the polymer filling and movement to the sample reservoir. (d) Electropherogram from an allelic ladder separation in the 7 cm microchip channel with five examples of 9.3–10 alleles for the TH01 marker showing one base pair resolution (expanded in red box).

fluidic movement. At this point, the stage is heated to the separation temperature for ME. Allelic ladder separations were performed to verify the resolution of this microchip and validate the ME. Fig. 5d shows a typical allelic ladder separation. The ME is able to resolve all of the peaks in the ladder to generate a binning matrix. TH01 9.3 and 10 are resolved to demonstrate that the system is able to discriminate the single base pair required by the forensic community for that multiplex kit (Fig. 5b left bottom corner). In addition, the size deviation calculation for each of the alleles for multiple allelic ladder comparison never exceeds ± 0.5 bp, demonstrating the precision of the ME.

Moreover, successful integrated PCR-ME full profiles were obtained, showing the DNA peaks and the size standard effectively separated (as shown in Fig. S6[†]). This verified sufficient mixing of the two liquids and good injection, separation and detection of all fragments. The allele calls from PCR-ME profiles were always concordant with the conventional results.

3.5. Integrated LE-PCR-ME

Successful LE-PCR-ME analyses of buccal swabs are shown in Fig. 6. Three different donors were tested for this

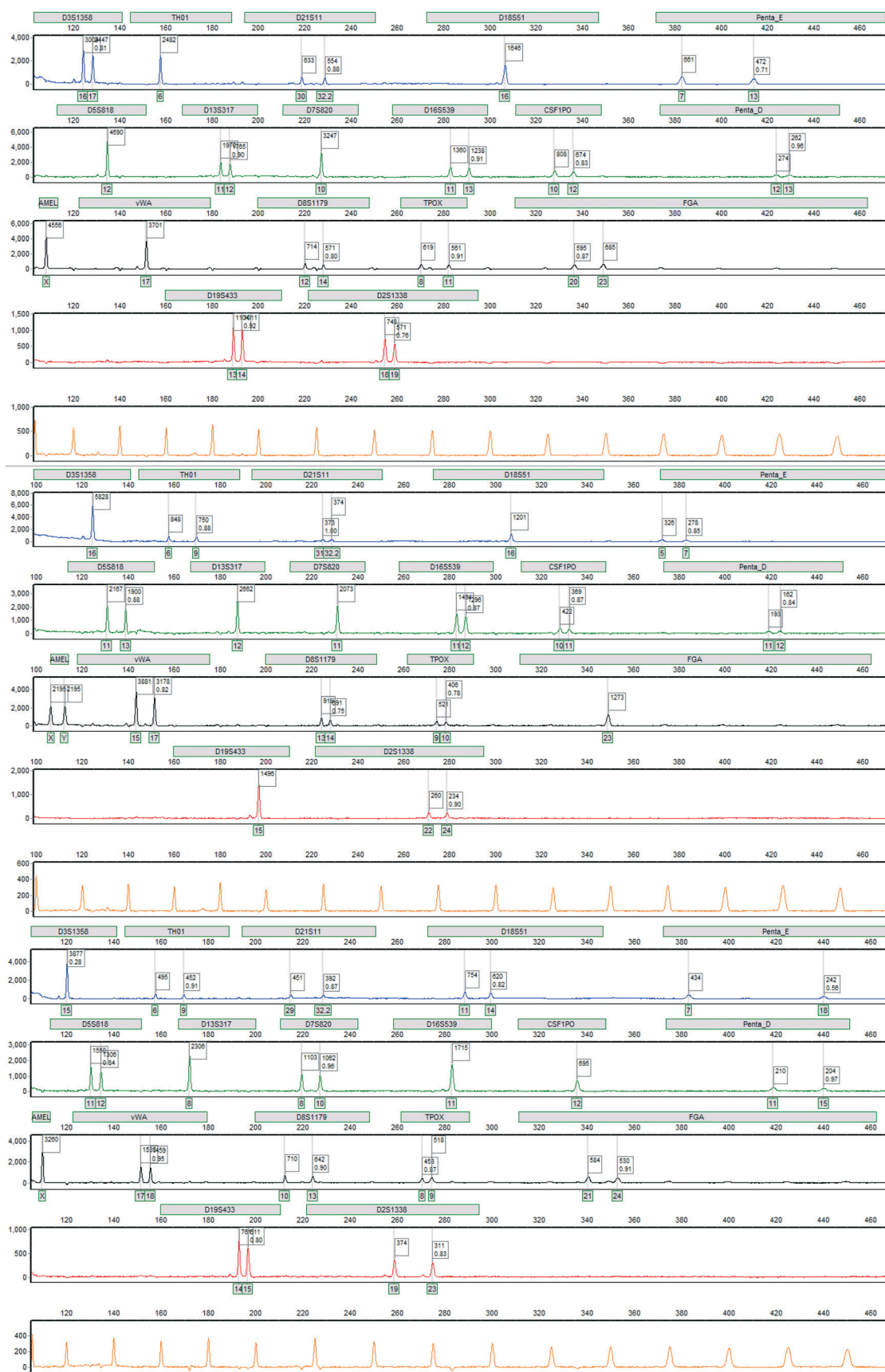


Fig. 6 Electropherograms of three different donors integrated with LE-PCR-ME. Allele calls are 100% concordant with conventional profiles.

preliminary demonstration of the fully integrated microfluidic chip for “sample-in-answer-out” human identification. The profiles show that each of the 18 loci was successfully amplified and separated with the internal lane standard. The alleles from the sample were analyzed using GeneMarker™ to call the allele numbers using a binning palette created from an allelic ladder separation run on the system under the same conditions. The allele calling was compared against the conventional method and found to be 100% concordant. Additionally, Fig. S7† shows the final donor in Fig. 6 analyzed for two additional times by the LE-PCR-ME microchip, demonstrating that the system is capable of reproducing the same profile. Therefore, full and concordant genetic profiles can be obtained by LE-PCR-ME on the microfluidic chip, as demonstrated here. Following this proof-of-principle demonstration, it will be of interest to perform forensic validation tests to evaluate the performance of the system for robustness, more challenging applications, and different sample types. An expert system capable of kinship analysis will be of interest in the next phase of development to demonstrate other applications.

4. Discussion

The advantages of a fully integrated μ TAS for forensic STR analysis are clear: (i) a fully enclosed microfluidic system reduces the opportunity for contamination from conventional liquid transfer steps, (ii) a simple work flow allows less experienced users to perform the analysis at the point-of-sample collection, and (iii) the analysis time is reduced substantially compared with the current process. While the sample-to-answer analytical time is reduced, the greater impact of these systems may be the time saved associated with eliminating the need to transport samples to a central laboratory for testing.

While other integrated DNA systems have been previously reported,^{28,29,31} it is important to note several critical features that distinguish the system described here. First, the main component of the microchip is a single injection-molded piece of Cyclo Olefin Polymer (COP). This significantly reduces the cost of fabrication compared with devices made from glass²⁸ or from multiple components.^{29,30} The final microchip assembly processes of sputtering electrodes, solvent bonding and lamination of the capping layers on to the flat chip are well established and can be easily scaled to larger batches of microchips. This straightforward fabrication process, along with no requirement for microchip surface pretreatment, enables a simple and low-cost fabrication process.

Second, this microchip has the footprint roughly the size of a 96-well plate and is capable of analyzing four samples simultaneously. This is a stark contrast to other reports for genetic analysis with similar high-resolution separation but using microfluidic devices that either have a substantially larger footprint, or involve multiple microdevices interfaced with a capillary array. The reduced size is enabled by two

different technologies. First, the unique hydrophobically modified polyacrylamide polymer enables the high-resolution DNA separation to be achieved in an effective length of 7 cm compared with other reports for similar assays with lengths of 22.5 cm in a plastic substrate,³¹ 14 cm in a glass substrate,²⁸ or in an off-the-shelf capillary.²⁹ Additionally, the enzyme preparation method allows footprint compression by eliminating the need for reagents required for chromatographic purification of DNA on solid phases and the reservoir for liquid waste (*e.g.*, adsorption, wash and elution buffers) as well as containing fewer fluidic transport channels. While this study has focused on forensic applications, the DNA preparation-PCR amplification-electrophoretic separation process can be extended to other diagnostics including clinical, environmental and food testing.

5. Conclusions

A fully integrated sample-in-answer-out microchip for human identification based on STR analysis was demonstrated. A combination of enzymatic DNA preparation, microliter PCR, and a unique separation polymer enabled a compact footprint and plastic microchip substrate and eliminated all surface pretreatments. The enzymatic DNA preparation with appropriate microfluidic movements leads to full genetic profiles from buccal brush swabs and buccal cells on FTA paper, showing that the system can be used for at least two different DNA inputs. An aliquot of this DNA sample allowed an 18-plex STR amplification that provides similar profiles to that of the conventional method. The PCR product was separated in an effective length of 7 cm using a polymer that resolves each of the peaks of the allelic ladder and achieved concordant and accurate allele calling for three different individuals. This proof-of-concept micro-total analysis system is a critical step towards achieving a low-cost microchip for a point-of-collection human identification system.

Acknowledgements

The authors are grateful for technical support from Michael E. Egan, Darren Albert and Douglas J. South from Lockheed Martin Corp, Bethesda, MD. We also thank Doug Storts from Promega Corporation for reagent improvements and supporting the development and Morpho for financial support. JPL acknowledges funding in grants from the National Institutes of Health – 5R01HG002613-03 and 5R01HG001832-07. Finally, the authors are especially grateful to the collaboration with MiniFAB, Victoria, Australia, for microfluidic chip design development and fabrication.

References

- 1 P.-A. Auroux, Y. Koc, A. deMello, A. Manz and P. J. R. Day, *Lab Chip*, 2004, 4, 534–546.
- 2 P. Lisowski and P. K. Zarzycki, *Chromatographia*, 2013, 76, 1201–1214.

- 3 A. K. Yetisen, M. S. Akram and C. R. Lowe, *Lab Chip*, 2013, **13**, 2210–2251.
- 4 M. Mascini and S. Tombelli, *Biomarkers*, 2008, **13**, 637–657.
- 5 D. Eicher and C. A. Merten, *Expert Rev. Mol. Diagn.*, 2011, **11**, 505–519.
- 6 L. Kulinsky, Z. Noroozi and M. Madou, *Methods Mol. Biol.*, 2013, **949**, 3–23.
- 7 D. Mark, S. Haeberle, G. Roth, F. von Stetten and R. Zengerle, *Chem. Soc. Rev.*, 2010, **39**, 1153–1182.
- 8 Y. Zhang and P. Ozdemir, *Anal. Chim. Acta*, 2009, **638**, 115–125.
- 9 C. W. Price, D. C. Leslie and J. P. Landers, *Lab Chip*, 2009, **9**, 2484–2494.
- 10 D. Wu, J. Qin and B. Lin, *J. Chromatogr. A*, 2008, **1184**, 542–559.
- 11 M. C. Breadmore, K. A. Wolfe, I. G. Arcibal, W. K. Leung, D. Dickson, B. C. Giordano, M. E. Power, J. P. Ferrance, S. H. Feldman, P. M. Norris and J. P. Landers, *Anal. Chem.*, 2003, **75**, 1880–1886.
- 12 D. Jungkind, *J. Clin. Virol.*, 2001, **20**, 1–6.
- 13 R. J. Mariella, *Biomed. Microdevices*, 2008, **10**, 777–784.
- 14 A. J. de Mello and N. Beard, *Lab Chip*, 2003, **3**, 11N–20N.
- 15 E. A. Oblath, W. H. Henley, J. P. Alarie and J. M. Ramsey, *Lab Chip*, 2013, **13**, 1325–1332.
- 16 I. Pjescic and N. Crews, *Lab Chip*, 2012, **12**, 2514–2519.
- 17 D. Chen, M. Mauk, X. Qiu, C. Liu, J. Kim, S. Ramprasad, S. Ongagna, W. R. Abrams, D. Malamud, P. L. A. M. Corstjens and H. H. Bau, *Biomed. Microdevices*, 2010, **12**, 705–719.
- 18 S. Nie, W. H. Henley, S. E. Miller, H. Zhang, K. M. Mayer, P. J. Dennis, E. A. Oblath, J. P. Alarie, Y. Wu, F. G. Oppenheim, F. F. Little, A. Z. Uluer, P. Wang, J. M. Ramsey and D. R. Walt, *Lab Chip*, 2014, **14**, 1087–1098.
- 19 A. F. Sauer-Budge, P. Mirer, A. Chatterjee, C. M. Klapperich, D. Chargin and A. Sharon, *Lab Chip*, 2009, **9**, 2803–2810.
- 20 K.-Y. Lien, C.-J. Liu, P.-L. Kuo and G.-B. Lee, *Anal. Chem.*, 2009, **81**, 4502–4509.
- 21 X. Pan, L. Jiang, K. Liu, B. Lin and J. Qin, *Anal. Chim. Acta*, 2010, **674**, 110–115.
- 22 B. S. Ferguson, S. F. Buchsbaum, T.-T. Wu, K. Hsieh, Y. Xiao, R. Sun and H. T. Soh, *J. Am. Chem. Soc.*, 2011, **133**, 9129–9135.
- 23 R. H. Liu, J. Yang, R. Lenigk, J. Bonanno and P. Grodzinski, *Anal. Chem.*, 2004, **76**, 1824–1831.
- 24 Z. Chen, W. R. Abrams, E. Geva, C. J. de Dood, J. M. González, H. J. Tanke, R. S. Niedbala, P. Zhou, D. Malamud and P. L. A. M. Corstjens, *BioMed Res. Int.*, 2013, **2013**, 543294.
- 25 J. M. Butler, *Fundamentals of Forensic DNA Typing*, Elsevier Science, 2009.
- 26 K. M. Horsman, J. M. Bienvenue, K. R. Blasier and J. P. Landers, *J. Forensic Sci.*, 2007, **52**, 784–799.
- 27 C. J. Easley, J. M. Karlinsey, J. M. Bienvenue, L. A. Legendre, M. G. Roper, S. H. Feldman, M. A. Hughes, E. L. Hewlett, T. J. Merkel, J. P. Ferrance and J. P. Landers, *Proc. Natl. Acad. Sci. U. S. A.*, 2006, **103**, 19272–19277.
- 28 P. Liu, X. Li, S. A. Greenspoon, J. R. Scherer and R. A. Mathies, *Lab Chip*, 2011, **11**, 1041–1048.
- 29 L. K. Hennessy, H. Franklin, Y. Li, J. Buscaino, K. Chear, J. Gass, N. Mehendale, S. Williams, S. Jovanovich, D. Harris, K. Elliott and W. Nielsen, *Forensic Sci. Int.: Genet.*, 2013, **4**, 7–8.
- 30 A. J. Hopwood, C. Hurth, J. Yang, Z. Cai, N. Moran, J. G. Lee-Edghill, A. Nordquist, R. Lenigk, M. D. Estes, J. P. Haley, C. R. McAlister, X. Chen, C. Brooks, S. Smith, K. Elliott, P. Koumi, F. Zenhausern and G. Tully, *Anal. Chem.*, 2010, **82**, 6991–6999.
- 31 E. Tan, R. S. Turingan, C. Hogan, S. Vasantgadkar, L. Palombo, J. W. Schumm and R. F. Selden, *Invest. Genet.*, 2013, 4–16.
- 32 D. Moss, S. A. Harbison and D. J. Saul, *Int. J. Legal Med.*, 2003, **117**, 340–349.
- 33 J. A. Lounsbury, N. Coult, D. C. Miranian, S. M. Cronk, D. M. Haverstick, P. Kinnon, D. J. Saul and J. P. Landers, *Forensic Sci. Int.: Genet.*, 2012, **6**, 607–615.
- 34 M. G. Roper, C. J. Easley, L. A. Legendre, J. A. C. Humphrey and J. P. Landers, *Anal. Chem.*, 2007, **79**, 1294–1300.
- 35 D. Le Roux, B. E. Root, C. R. Reedy, J. A. Hickey, O. N. Scott, J. M. Bienvenue, J. P. Landers, L. Chassagne and P. de Mazancourt, *Anal. Chem.*, 2014, **86**, 8192–8199.
- 36 K. Oostdik, J. French, D. Yet, B. Smalling, C. Nolde, P. M. Vallone, E. L. R. Butts, C. R. Hill, M. C. Kline, T. Rinta, A. M. Gerow, S. R. Allen, C. K. Huber, J. Teske, B. Krenke, M. Ensenberger, P. Fulmer and C. Sprecher, *Forensic Sci. Int.: Genet.*, 2013, **7**, 129–135.